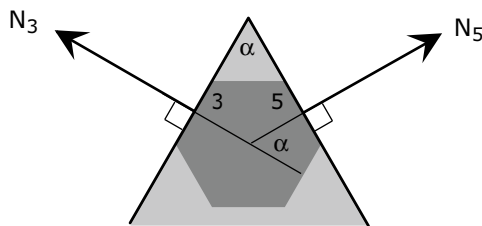


## Some Crystallography

In the previous chapter we saw how to calculate the radii of circular halos from the wedge angles (interfacial angles) on a crystal. In the present chapter we will see how to calculate the likely wedge angles from crystallographic principles and from the  $c/a$  ratio of ice. The crystallographic principles together with the  $c/a$  ratio therefore determine the likely halo radii. Not everyone will find this chapter to be easy going. If this applies to you, you can of course skip the work and just take the results on faith. There are two of them. First, on a pyramidal crystal the angle of inclination  $x$  of the pyramid faces to the crystal axis determines all of the wedge angles on the crystal. Second, the most likely value of  $x$  is  $28^\circ$ . The first statement should seem plausible, perhaps obvious. But the second statement will be hard to swallow—and impossible to appreciate—unless you attempt to follow the reasoning of this chapter.

### Wedge angles from angle $x$

It is easy to calculate the wedge angle of a wedge if the normal vectors to the two wedge faces are known. In Figure 9.1, for example, the wedge angle is the supplement of the angle between the outward normal vectors  $\mathbf{N}_3$  and  $\mathbf{N}_5$ , or, equivalently, it is the angle between  $-\mathbf{N}_3$  and  $\mathbf{N}_5$ .



**FIGURE 9.1** Like Figure 8.7 but with the addition of  $\mathbf{N}_3$  and  $\mathbf{N}_5$ , the normal vectors to faces 3 and 5. The wedge angle  $\alpha$  is equal to the angle between  $-\mathbf{N}_3$  and  $\mathbf{N}_5$ .

In general,

$$\cos \alpha = -\frac{\mathbf{N}_i \cdot \mathbf{N}_j}{|\mathbf{N}_i| |\mathbf{N}_j|}, \tag{9.1}$$

where  $\alpha$  is the wedge angle for entry and exit faces  $i$  and  $j$ , and where  $\mathbf{N}_i$  and  $\mathbf{N}_j$  are the outward normal vectors to the two faces.

We said that the inclination angle  $x$  determines all wedge angles on a pyramidal crystal. For the wedge 13 14, for example, here is how to calculate its wedge angle in terms of  $x$ :

With the crystal axis vertical, as in Figure 9.2, angle  $x$  is not only the inclination of the pyramid faces to the crystal axis, it is also the inclination of their normal vectors to the horizontal plane. The outward normal vector  $\mathbf{N}_{13}$  to face 13 can therefore be written

$$\mathbf{N}_{13} = (\cos t \cos x, \sin t \cos x, \sin x), \tag{9.2}$$

where  $t$  is the azimuth of the vector. Here we have temporarily assumed the face normals to have unit length.

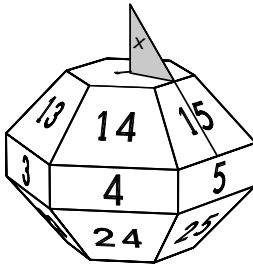


**FIGURE 9.2** (Above) Pyramidal crystal illustrating angle  $x$ , that is, the angle of inclination of the pyramid faces to the crystal axis. Angle  $x$  determines all wedge angles of the crystal (Table 9.1). Here  $x = 39^\circ$ , which turns out to be unrealistic.

Wedge faces	$\cos \alpha$
13 6	$\cos x$
13 25	$(3 - \cos 2x)/4$
13 16	$\cos 2x$
3 5	$1/2$
13 2	$\sin x$
13 5	$(\cos x)/2$
13 15	$(-1 + 3 \cos 2x)/4$
1 3	0
13 24	$-(-1 + 3 \cos 2x)/4$
13 4	$-(\cos x)/2$
13 1	$-\sin x$
3 4	$-1/2$
13 23	$-\cos 2x$
13 14	$-(3 - \cos 2x)/4$
13 3	$-\cos x$

**TABLE 9.1** (Right) Wedge angles  $\alpha$  on a pyramidal crystal having inclination angle  $x$  (Figure 9.2). For each wedge the table gives  $\cos \alpha$  in terms of  $x$ . The last seven wedge angles are supplements of the first seven but in reverse order. The wedge angle values in Table 8.1 result from this table by taking  $x = 28^\circ$ .

You can get  $\mathbf{N}_{14}$  by rotating  $\mathbf{N}_{13}$  through an angle of  $60^\circ$  about the vertical axis, that is, you increase its azimuth by  $60^\circ$ , so

$$\mathbf{N}_{14} = (\cos(t + 60) \cos x, \sin(t + 60) \cos x, \sin x) \quad (9.3)$$

Hence from Eqs. (9.1), (9.2), (9.3), the wedge angle  $\alpha$  is given by

$$\begin{aligned} \cos \alpha &= -\mathbf{N}_{13} \cdot \mathbf{N}_{14} \\ &= -\frac{1}{2} (\cos^2 x + 2 \sin^2 x) \\ &= \frac{1}{4} (-3 + \cos 2x) \end{aligned} \quad (9.4)$$

The remaining wedge angles are computed similarly and are listed in Table 9.1.

### Angle $x$ from crystallography

We now explain how the principles of crystallography limit the possibilities for  $x$ . Proofs and more explanation are given in Appendix E.

Ice is a mineral and is therefore expected to conform to the principles of crystallography. A crystal of any mineral has an internal 3-dimensional lattice which, mathematically, consists of all points that are integral linear combinations of three independent vectors  $\mathbf{v}_1$ ,  $\mathbf{v}_2$ ,  $\mathbf{v}_3$ . The three vectors  $\mathbf{v}_1$ ,  $\mathbf{v}_2$ ,  $\mathbf{v}_3$  are said to be a *basis* for the lattice. For minerals like ice that have hexagonal symmetry the lattice and lattice basis are as shown in Figure 9.3; the vectors  $\mathbf{v}_1$  and  $\mathbf{v}_2$  are of length  $a$  and make an angle of  $120^\circ$  with each other, and the vector  $\mathbf{v}_3$  is of length  $c$  and is perpendicular to both  $\mathbf{v}_1$  and  $\mathbf{v}_2$ . The parameters  $a$  and  $c$  depend on the mineral.

A fundamental tenet of crystallography is that on a crystal of a given mineral only certain crystal faces are possible: For a plane to be a crystal face, it must be a lattice plane, that is, it must contain three non-collinear lattice points. Furthermore, of all the lattice planes, only a small fraction of them are really likely to be crystal faces. How, then, can you recognize a lattice plane, and how can you tell when it is likely to be a crystal face?

Associated with the lattice basis  $\mathbf{v}_1$ ,  $\mathbf{v}_2$ ,  $\mathbf{v}_3$  is the so-called dual basis  $\mathbf{w}^1$ ,  $\mathbf{w}^2$ ,  $\mathbf{w}^3$ . Whereas the lattice basis is naturally suited to handle lattice points, the dual basis is suited to handle lattice planes. Any plane not containing the origin has an outward normal vector  $\mathbf{N}$  which, like any vector, can be expressed as a linear combination of the dual basis vectors:

$$\mathbf{N} = h\mathbf{w}^1 + k\mathbf{w}^2 + l\mathbf{w}^3 \quad (9.5)$$

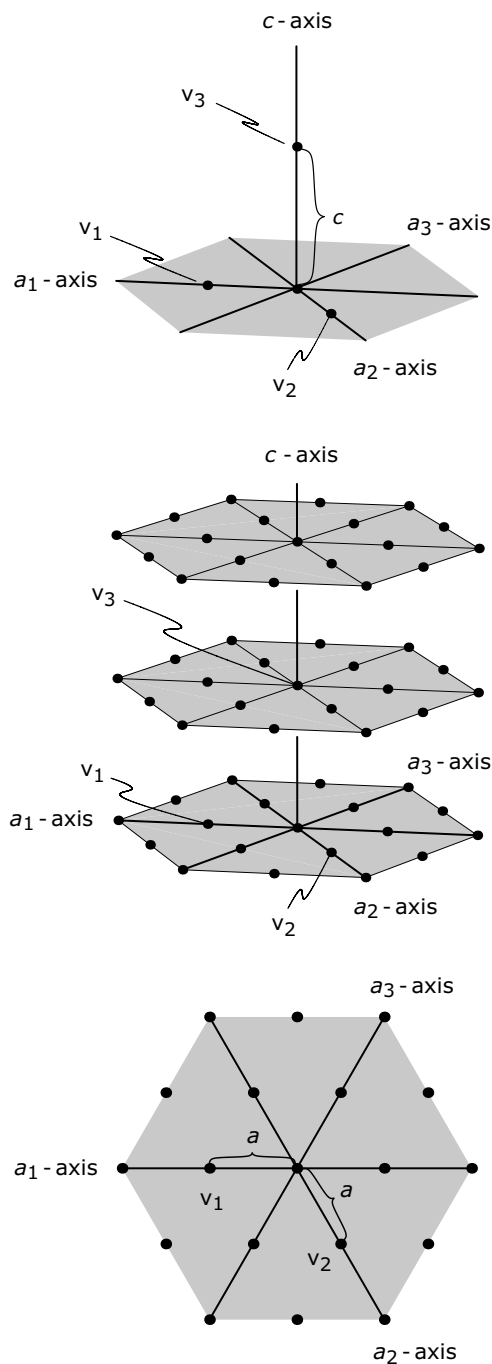


**FIGURE 9.3** (Top) Lattice basis  $\mathbf{v}_1$ ,  $\mathbf{v}_2$ ,  $\mathbf{v}_3$  for ice. The  $a_1$ ,  $a_2$ ,  $a_3$ , and  $c$ -axes are in the directions of  $\mathbf{v}_1$ ,  $\mathbf{v}_2$ ,  $-(\mathbf{v}_1 + \mathbf{v}_2)$ , and  $\mathbf{v}_3$ , respectively; thus it is the  $c$ -axis, rather than the  $a_3$ -axis, that is in the direction of  $\mathbf{v}_3$ . (Middle) Same but showing the lattice as well as the lattice basis. The lattice consists of the lattice points (heavy dots), which are understood to extend indefinitely in all directions. (Bottom) The bottom section of the middle diagram but as seen from directly above, looking down the  $c$ -axis.

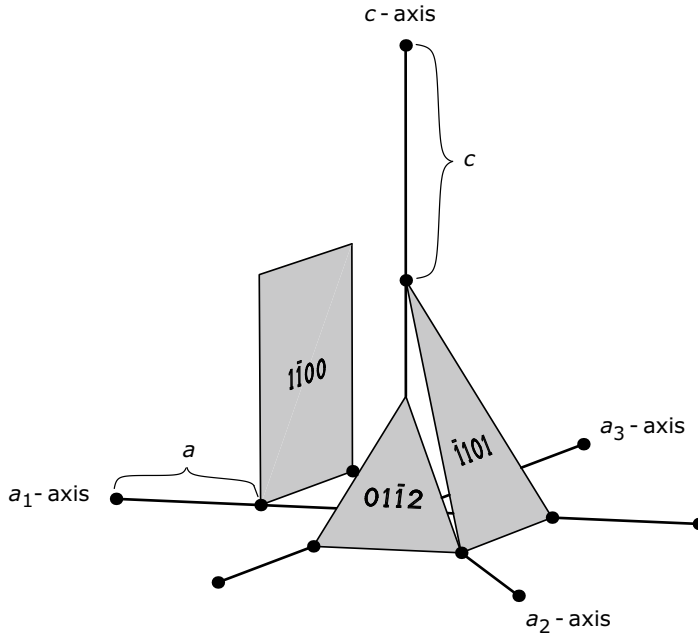


**FIGURE 9.4** Lattice planes with Miller indices  $1\bar{1}00$ ,  $\bar{1}101$ , and  $01\bar{1}2$ . The  $01\bar{1}2$  plane, for example, is parallel to the  $a_1$ -axis and intersects the  $a_2$ ,  $a_3$ , and  $c$ -axes at  $a/1$ ,  $a/(-1)$ , and  $c/2$ , the denominators of these fractions being the Miller indices. In all of Figures 9.3–9.10, the  $c/a$  ratio is 1.63; this is the modern  $c/a$  value for ice, the same as that found by Barnes (Chapter 7).

for some real numbers  $h, k, l$ . If the plane is a lattice plane—and hence a possible crystal face—it turns out that  $h, k, l$  are relatively prime integers, that is, whole numbers with no common factors.<sup>1</sup> And although there is a lattice plane for each triple of relatively prime integers  $h, k, l$ , that is, there is a lattice plane with normal vector  $\mathbf{N}$  given by Eq. (9.5), only the lattice planes with  $h, k, l$  small are at all likely to be crystal faces. The integers  $h, k, l$  are the *Miller indices* of the face. They are usually written without commas, and with negative integers indicated by overbars instead of minuses, so that, for example, the Miller indices 1, 2,  $-2$  would be written  $12\bar{2}$ .

To get some geometric feeling for Miller indices, you need to know that the plane containing the three points  $(1/h)\mathbf{v}_1$ ,  $(1/k)\mathbf{v}_2$ , and  $(1/l)\mathbf{v}_3$  is a lattice plane with Miller indices  $hkl$ . Three examples are shown in Figure 9.4.

<sup>1</sup> More correctly, the length of  $\mathbf{N}$  can be adjusted so that  $h, k, l$  become relatively prime integers.

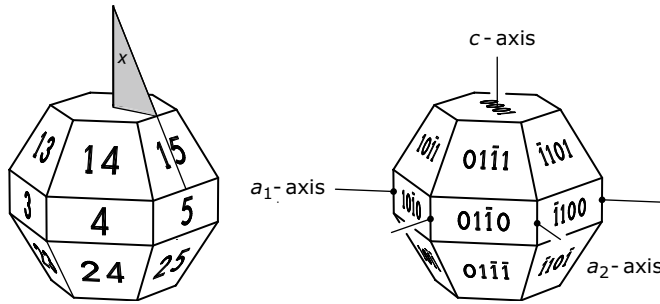


**FIGURE 9.5** (Left) Standard pyramidal ice crystal as hypothesized by Steinmetz and Weickmann (same as Figure 8.2). The crystal has prism, basal, and  $\{10\bar{1}1\}$  pyramid faces. The angle  $x$  is  $28^\circ$  [Eq. (9.6) with  $c/a = 1.63$  and  $h = l = 1$ ]. (Right) Same crystal but with the faces identified by their Miller indices.

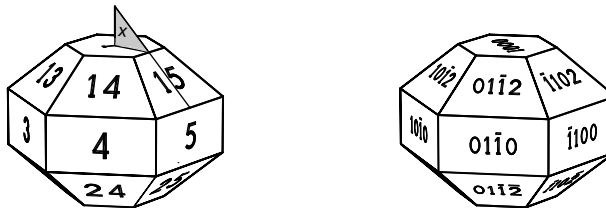


**FIGURE 9.6** Like Figure 9.5 but with  $\{10\bar{1}2\}$  faces instead of  $\{10\bar{1}1\}$  faces. The angle  $x$  is now  $46.7^\circ$ .

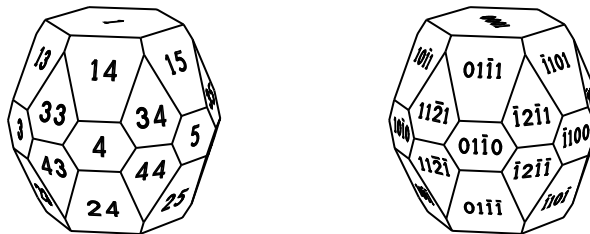


**FIGURE 9.7** Like Figure 9.5 but with the addition of  $\{11\bar{2}1\}$  faces, the simplest second order pyramid faces.

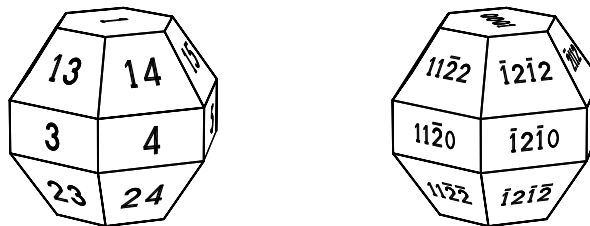


**FIGURE 9.8** Crystal easily mistaken for that in Figure 9.5. The crystal has basal faces,  $\{11\bar{2}0\}$  prism faces, and  $\{11\bar{2}2\}$  pyramid faces. Angle  $x$  is  $31.5^\circ$ . In all figures on this page the crystallographic axes are oriented the same; here each  $a$ -axis is perpendicular to a (second order) prism face.

For minerals like ice that have hexagonal symmetry there are good geometrical reasons for replacing the triple of Miller indices  $hkl$  with the 4-tuple  $hkil$ , where  $i = -(h+k)$ . We will usually do so, as in Figure 9.4. This corresponds to introducing another axis, the  $a_3$ -axis, as shown in the figure. The  $a_1$ ,  $a_2$ , and  $c$ -axes are in the directions of  $\mathbf{v}_1$ ,  $\mathbf{v}_2$ ,  $\mathbf{v}_3$ , while the  $a_3$ -axis is in the direction of  $-(\mathbf{v}_1 + \mathbf{v}_2)$ .

Each crystal face is part of what is known as a crystallographic form. The form is the collection of faces related to the given face by the internal symmetries of the crystal.<sup>2</sup> Curly brackets distinguish the form from the face. That is,  $\{hkl\}$  is the form containing the face  $hkl$ . In Figure 9.5 the  $\{0001\}$  form consists of the two basal faces, and the  $\{10\bar{1}0\}$  form consists of the six prism faces. The  $\{10\bar{1}1\}$  form consists of the twelve inclined faces. Technically the  $\{10\bar{1}1\}$  form is a hexagonal dipyramid, but we nevertheless refer to its faces as pyramid faces. (The crystal at the right in Figure 7.1 consists of a single dipyramid.)

The faces  $\{h0\bar{h}l\}$  and  $\{hh\bar{2}hl\}$  are known as first order and second order faces, respectively. They are prism faces if  $l = 0$  and they are (di-)pyramid faces otherwise. The crystals in Figures 9.5 and 9.6 have first order prism and pyramid faces, and the crystal in Figure 9.8 has second order prism and pyramid faces. The crystal in Figure 9.7 has first order prism faces, and it has both first and second order pyramid faces. Perhaps from Figures 9.9 and 9.10 you can see the somewhat subtle difference between first and second order faces. It is a difference that has plagued halo theory historically.

---

There has been a lot to absorb here. The main point is that crystallography gives us an idea of what crystal faces to expect—they are the lattice planes with small Miller indices.

What, then, can we expect for the faces on a real ice crystal? That is, what might their Miller indices be? All else being equal, we would expect the most common faces to be the  $\{0001\}$ ,  $\{10\bar{1}0\}$ , and  $\{10\bar{1}1\}$  faces. The  $\{0001\}$  and  $\{10\bar{1}0\}$  faces are of course the familiar basal and prism faces, and they are indeed common. The  $\{10\bar{1}1\}$  faces have to be our tentative first choice for the inclined faces. Other top candidates for the inclined faces would be the  $\{10\bar{1}2\}$  and  $\{11\bar{2}1\}$  faces. Again see Figures 9.5–9.7.

We are now close to being able to guess the wedge angles on a real pyramidal ice crystal.

---

<sup>2</sup> For ice there are 24 such symmetries. With the  $c$ -axis vertical, there are six rotations about the vertical axis, six reflections in vertical planes, and then each of the preceding twelve operations followed by reflection in the horizontal plane. The group of these 24 symmetries is often denoted by its Hermann–Mauguin symbol  $6/m\ 2/m\ 2/m$ .

**Angle  $x$  from Miller indices** *The inclination angle  $x$  between the  $\{hkl\}$  faces ( $h+k+i=0$ ) and the crystal axis is given by*

$$\tan x = \frac{\sqrt{3}}{2} \frac{a}{c} \left| \frac{l}{h} \right| \quad \text{if } k = 0 \quad (\text{first order faces}) \quad (9.6)$$

$$\tan x = \frac{1}{2} \frac{a}{c} \left| \frac{l}{h} \right| \quad \text{if } h = k \quad (\text{second order faces}) \quad (9.7)$$

See Figures 9.9 and 9.10.

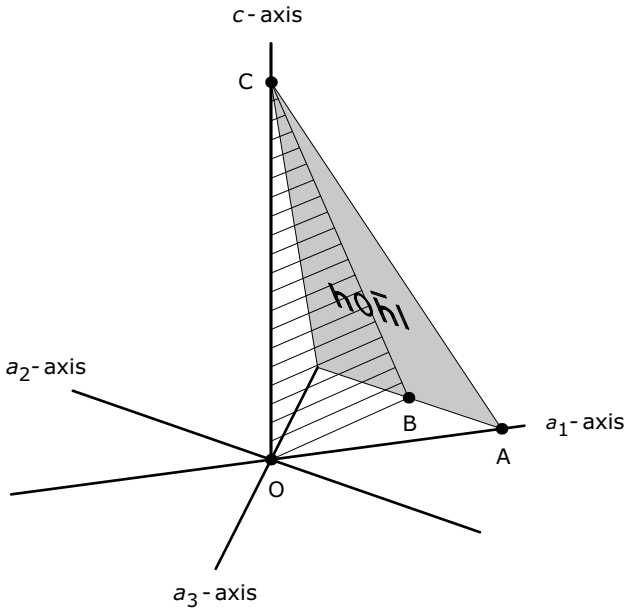
---

Bravais, who was one of the pioneers of crystallography, knew all of this a century and a half ago. That is, he was aware of something like our Table 9.1 and Eqs. (9.6) and (9.7). But to calculate the wedge angles on a pyramidal ice crystal, he still needed to know  $x$ , or he needed to know  $c/a$  together with the Miller indices of the pyramid faces. Not knowing  $c/a$ , he used a value of  $x$  inferred from Clarke's observation of rhombohedral crystals (Chapters 7 and 11). We now think this was a mistake. Much later, Steinmetz and Weickmann calculated the wedge angles differently. Using Barnes'  $c/a = 1.63$  and taking  $h = l = 1$  in Eq. (9.6), they calculated  $x = 28^\circ$ . In conjunction with Table 9.1, this then gives the wedge angle values listed in Table 8.1. This is our approach as well. In short, the wedge angles in Table 8.1 are calculated from the  $c/a$  ratio of ice by assuming that the pyramid faces are the  $\{10\bar{1}1\}$  faces.

What about some of the other crystallographically likely faces? We will see in the next chapter that the Steinmetz–Weickmann value  $x = 28^\circ$  looks about right for most real ice crystals. The  $\{10\bar{1}2\}$  faces and the  $\{11\bar{2}1\}$  faces, mentioned above as being candidates for the inclined faces, have  $x = 46.7^\circ$  and  $x = 17.1^\circ$ , respectively, and neither gives a crystal shape resembling the shape of real ice crystals. In fact, as can be seen from Table E.2 of Appendix E, the only plausible alternatives to the  $\{10\bar{1}1\}$  faces of Steinmetz and Weickmann are the  $\{11\bar{2}2\}$  faces, for which  $x = 31.5^\circ$ . These Miller indices are small enough to deserve consideration, and the resulting crystal shape (Figure 9.8) and halos are not so different from those for the  $\{10\bar{1}1\}$  faces. Careful observations, however, will distinguish the two possibilities, and the observations favor the  $\{10\bar{1}1\}$  faces, especially if one looks at the halos arising in preferentially oriented crystals.

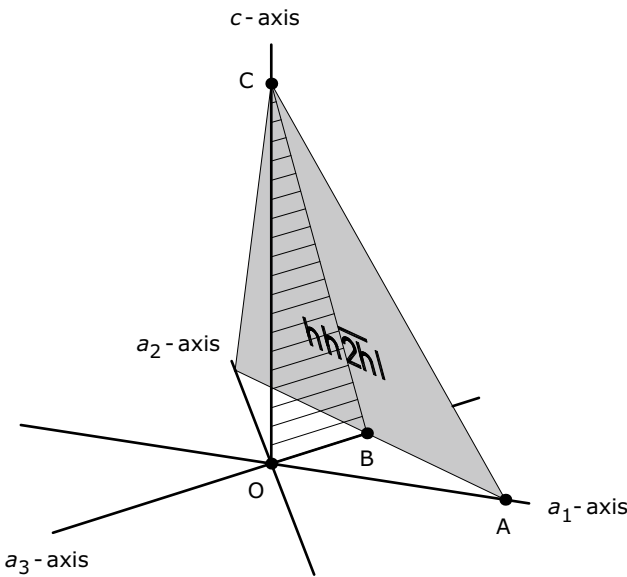
So we believe that Steinmetz and Weickmann were right and that the pyramid faces on ice crystals are normally the  $\{10\bar{1}1\}$  faces. If so, then the situation is complicated enough. But consider what it might have been. There seems to be no a priori reason why ice crystals should not exhibit other faces. Conceivably we could have had ice crystals like the one in Figure 9.7, for example, which has  $\{10\bar{1}1\}$  and  $\{11\bar{2}1\}$  pyramid faces in addition to the usual prism and basal





$$\begin{aligned} \tan x &= \tan \angle OCB \\ &= \frac{|\mathbf{OB}|}{|\mathbf{OC}|} \\ &= \frac{\sqrt{3}}{2} \frac{|\mathbf{OA}|}{|\mathbf{OC}|} \\ &= \frac{\sqrt{3}}{2} \frac{a}{c} \frac{l}{h} \end{aligned}$$

**FIGURE 9.9** Derivation of Eq. (9.6), which gives the inclination angle  $x$  for first order faces. The grey triangle is the  $h0\bar{h}l$  face; it is parallel to the  $a_2$ -axis and intercepts the  $a_1$ ,  $a_3$ , and  $c$ -axes at  $a/h$ ,  $a/(-h)$ , and  $c/l$ , the denominators of the fractions being given by the Miller indices as usual. Thus  $|\mathbf{OA}| = a/h$  and  $|\mathbf{OC}| = c/l$ . Since  $\angle \mathbf{OAB} = 60^\circ$ , the derivation proceeds as at the right.



$$\begin{aligned} \tan x &= \tan \angle OCB \\ &= \frac{|\mathbf{OB}|}{|\mathbf{OC}|} \\ &= \frac{1}{2} \frac{|\mathbf{OA}|}{|\mathbf{OC}|} \\ &= \frac{1}{2} \frac{a}{c} \frac{l}{h} \end{aligned}$$

**FIGURE 9.10** Derivation of Eq. (9.7), which gives  $x$  for second order faces. The grey triangle is the  $hh2\bar{h}l$  face; it intercepts the  $a_1$ ,  $a_2$ ,  $a_3$ , and  $c$ -axes at  $a/h$ ,  $a/h$ ,  $a/(-2h)$ , and  $c/l$ . Thus  $|\mathbf{OA}| = a/h$  and  $|\mathbf{OC}| = c/l$ , the same as in Figure 9.9, but now  $\angle \mathbf{OAB} = 30^\circ$ .

faces. Most halo theorists have never worried about such crystals, and indeed no such ice crystals have been recognized unequivocally, at least not among crystals formed in the open atmosphere. But some depth hoar crystals, which grow within the snowpack, have been reported to have highly exotic faces [16]. And there are other minerals, such as beryl, which have hexagonal symmetry similar to that of ice, and which sometimes come in complicated crystals. It could have been the same for the ice crystals that make halos.

Incidentally, if it *had* been the same, you could still have computed the wedge angles on the crystals, so long as you knew the Miller indices of the faces. [Use Eqs. (9.1), (9.5), and (E.11).] And once you have the wedge angles, you have the halo radii.

Before moving on, we invite you to look again at the figures from this chapter, if you are not yet comfortable with Miller indices. In all of Figures 9.4–9.8 the crystallographic axes are oriented identically and the  $c/a$  ratios are the same, so that faces with the same Miller indices are oriented identically when they appear in different figures. Thus the  $\bar{1}101$  face, which is face 15 in Figures 9.5 and 9.7, looks the same both in those figures and in Figure 9.4. The  $01\bar{1}2$  face, which is face 14 in Figure 9.6, looks the same there and in Figure 9.4.